This is a peer-reviewed, accepted author manuscript of the following research article:
Zhang, T., & Xu, L. (2022). Grid forming control for solid-state transformer operating in islanding and grid connected conditions.
In 11th International Conference on Power Electronics, Machines and Drives (PEMD 2022) IET. https://doi.org/10.1049/icp.2022.1053

GRID FORMING CONTROL FOR SOLID-STATE TRANSFORMER OPERATING IN ISLANDING AND GRID CONNECTED CONDITIONS

Taibo Zhang*, Lie Xu

Department of Electronic and Electrical Engineering, University of Strathclyde, Glasgow, UK
**taibo.zhang@strath.ac.uk*

Keywords: SOLID-STATE TRANSFORMER, CNOP, DROOP CONTROL, GRID FORMING.

Abstract

Solid-state transformer (SST) has recently been considered as one of the key components for future distribution networks with enhanced controllability and operating flexibility. This paper proposes a universal control scheme for SST's low voltage DC/AC converter such that the same grid forming control structure can be used during both islanding operation and grid connected state to the adjacent feeder through the conventional normally open point (CNOP). This ensures smooth transition between different operation states without the need for control mode switching. To reduce the coupling between active and reaction power, an additional compensation control using active and reactive power feedforward compensation to dq-axis current components of the DC/AC converter is proposed. Simulation results are provided to confirm the overall SST performance and effectiveness of the proposed control schemes during power reference changes when the SST is operated in grid connected mode through CNOP.

1 Introduction

The increasing penetration of the DERs has introduced new challenges to the distribution network, such as power quality, stability, reliability, etc [1]. These necessity upgrade of the distribution network to achieve more steady and reliable operation [2]. Among the power electronics solutions for tackling the challenges [3, 4], the solid-state transformer (SST) is considered as one of promising solutions. SST is a power electronics-based transformer which achieves AC/AC voltage conversion. Compared with the line-frequency transformer (LFT), SST can not only feature full controllability of voltage and power in the LV network, but also provide the potential DC connectivity at the middle stage and fault isolation capability between MV and LV networks [5].

SST has been explored to provide extensive service in the distribution network, such as DER integration [5], Static Compensators (STATCOMs) [6], dynamic voltage restorer (DVR) [7]. etc. For flexible network reconfiguration to improve system availability, resilience and reliability [8], replacing LFT with SST and working compared with the conventional normally open point (CNOP) enables more efficient usage of network capacity by accurately regulating power flow.

Depending on the state of the CNOP and LV side network configuration, SST needs operate with either grid forming or grid following mode [8-10]. In [9], the SST is designed to interlink the LVAC and LVDC network, where only the voltage control is applied at DC/AC stage of SST to supply LVAC loads. The DC/AC converter of SST in [10] is only designed for grid forming operation to provide stabilised AC supply to AC microgrids without considering the CNOP connection. In [8], control schemes of SST under grid forming and grid following operation are presented separately, where the switch of the control schemes has yet to be studied. In addition, with droop control under grid following operation, a 0.4 pu change of reactive power could result in 20% variation of the active power output, which needs further improvement. To address some of the SST control problems of the LV side converter, a universal control scheme using a grid forming structure is proposed in this paper which can operate when the LV side operates either as an isolated network or grid connected to the adjacent network (through the CNOP). To address the coupling issue between active and reactive power with the grid forming control design when the SST LV side is grid connected, an additional compensation scheme is proposed.

The rest of this paper is organised as follows. The configuration of the tested SST-based distribution network is presented in Section 2, and the basic control of SST is presented in Section 3. The grid forming control scheme is presented in Section 4, while the simulation results are illustrated in Section 5 to show the performance of the proposed control schemes. Finally, Section 6 concludes this paper.

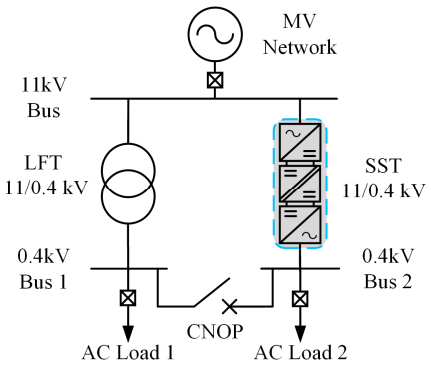

Fig. 1 Tested network with SST integration.

2 System Configuration

Fig. 1 illustrates an example distribution network where an SST replaces a normal line frequency transformer (LFT) in one of the feeders and the use of the CNOP for connections at the LV networks. As seen, AC Load 1 and AC Load 2 are connected to the 11 kV feeder, via the conventional LFT and SST, respectively. The CNOP is installed between the 0.4 kV Bus 1 and Bus 2. The SST considered contains three stages, including an AC/DC, DC/DC and DC/AC converter stages. SST can supply AC Load 2 on its own (as an island) while can also facilitate smooth connection and disconnection of the CNOP. When the CNOP is closed, the power transfer through CNOP can also be actively controlled by SST, thus the power dispatch to AC Load 1 and AC Load 2 can be optimised.

3 Basic Control of SST

The overall control scheme of the SST is shown in Fig. 2. For the stage 1 AC/DC converter, it is designed to regulate the MVDC voltage and its control is similar to that of the DC voltage controlling terminal in a VSC HVDC transmission system [11]. The stage 2 DC/DC converter is designed to convert DC voltage levels from MV to LV and regulate the DC voltage at the LV side. The stage 3 DC/AC converter is designed to either establish/form the voltage and frequency of the LVAC grid (when CNOP opens) or regulate the transmitted power to the LV AC network (when CNOP closes).

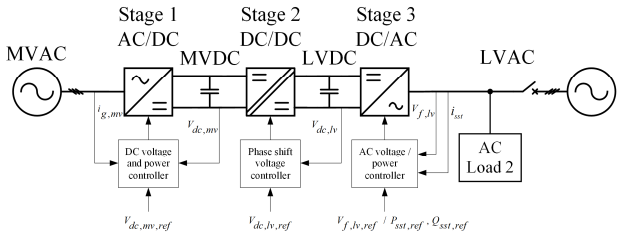

Fig. 2 Overall control scheme of the three stage SST.

3.1. Stage 1 AC/DC converter

The MVDC voltage and reactive power (MVAC side) are regulated by the AC/DC converter. As such control is well understood, only a brief introduction is provided here. A dual-loop control system, including an outer DC voltage loop and an inner current loop are used. Considering the inner current dynamics under synchronous dq frame aligned to the MVAC network voltage, the inner current control loop can be designed which generate the reference voltages for the AC/DC converter output. To control the DC voltage, an outer DC voltage control loop is designed which generates the d-axis (active) current reference for the inner current control loop. The q-axis (reactive) current order can be set according to the required SST operating power factor. Fig. 3 shows the overall block diagram for the AC/DC converter control.

3.2 DC/DC converter

The control objective of the DC/DC converter is to regulate the DC voltage at the LV side and the detailed control scheme is determined by the selected DC/DC converter topology. When the dual active bridge is used, the power transferred by phase shift modulation (PSM) can be derived as [12]:

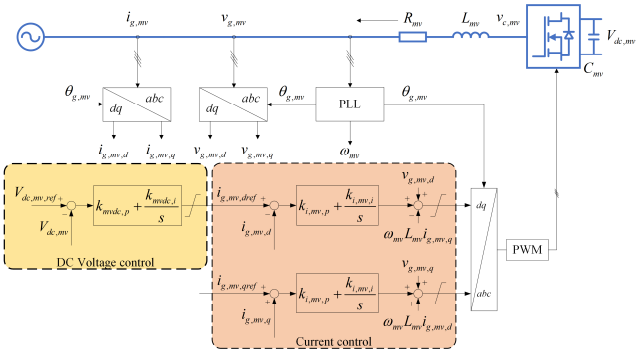

Fig. 3 Control scheme for AC/DC converter.

$$P_{DAB} = \frac{V_{dc,mv} n V_{dc,lv}}{2 f_s L_{DAB}} D(1-D) \tag{1}$$

where f_s is the switching frequency, $V_{dc,lv}$ is the LVDC voltage. n is the transformer ratio, and D is the phase shift ratio between the two voltages, defined as $D = \varphi/\pi$, where φ is the phase shift angle. Again the concept is well understood so no further details are provided here. An example control scheme for regulating LVDC voltage can be achieved by applying a PI controller, as illustrated in Fig. 4.

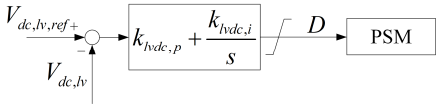

Fig. 4 Control scheme for DC/DC converter

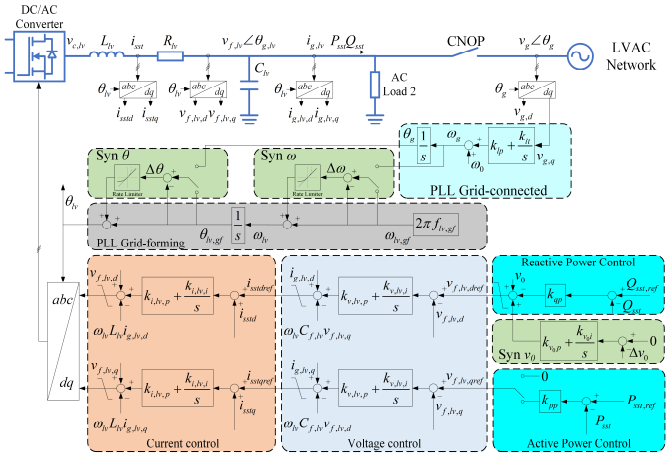

Fig. 5 Control scheme for DC/AC converter.

3.3 DC/AC converter

Depending on the network state (CNOP state), the operation mode of the DC/AC converter can be significantly different. It is anticipated that most of the time the SST will supply power to AC Load 2 with CNOP disconnected. Thus the DC/AC converter will be operated under grid forming mode to establish the LVAC grid with defined voltage amplitude and frequency. However, in the event when the CNOP is closed, the DC/AC converter is supplied to an external AC source and the operation mode needs to change to grid following with pre-defined active and reactive power setting point. The design also needs to consider the transient for the connecting and disconnecting of the CNOP. In order to facilitate smooth operation and transients between different operation modes, a universal control design is adopted here where grid forming

with active and reactive power references is implemented regardless whether the CNOP is closed or not. The control scheme of the DC/AC converter consists of current control, voltage control, active and reactive power control, synchronization control etc., as illustrated in Fig. 5, and some of the details are discussed in Section 4.

4. Grid Forming Control

As illustrated in Fig. 5, the control structure of the DC/AC converter consists many different blocks. However, due to space limitation, this paper will focus on active and reactive power control while grid forming structure is adopted. Specifically, it addresses the coupling issue between active and reactive power and the proposal of a compensation strategy.

4.1 AC current and voltage control

The grid forming structure adopted here contains the well-defined inner AC current and AC voltage control loops, enabling fast response and current limiting during external AC fault [11]. The detailed designs of such control loops are well-understood so no further description is provided here.

4.2 Active and reactive power control

Active and reactive power control scheme for SST is specifically required when the CNOP is closed and the LV side is grid connected. As previously described, in order to avoid control mode switching during the ON and OFF of CNOP, a universal grid forming approach is adopted for both operation conditions. The droop control is widely applied for active and reactive power control due to its better reliability and avoidance of communication links. The principle of the droop control is to adjust the output voltage and frequency in functions of active and reactive power delivered by the inverter [13]. Considering the inductive line impedance, the active and reactive power can be controlled by angular frequency and voltage magnitude difference between inverter output voltage $v_{f,lv}$ and the grid voltage v_g. The conventional P - ω and Q - v droop control can be derived as:

$$\omega_{lv,ref} - \omega_{lv} = -k_p \left(P_{sst,ref} - P_{sst} \right) \tag{2}$$

$$v_{f,lv,ref} - v_{f,lv} = -k_{qp} \left(Q_{sst,ref} - Q_{sst} \right) \tag{3}$$

where ω_{lv} and $\omega_{lv,ref}$ are the real and rated value of the DC/AC converter angular frequency. $v_{f,lv}$ and $v_{f,lv,ref}$ are real and rated value of the DC/AC converter output voltage amplitude. P_{sst} and $P_{sst,ref}$ are the real and reference active power, whilst Q_{sst} and $Q_{sst,ref}$ the real and reference reactive power of the SST. k_{qp} and k_p are the droop coefficients, respectively. The selection of the droop coefficients needs to be designed properly since they make an influence on the network stability. Generally, the droop coefficients can be estimated as:

$$k_p = \frac{\Delta\omega}{2P_{\max}}, k_{qp} = \frac{\Delta v}{2Q_{\max}} \tag{4}$$

where $\Delta\omega$ and Δv are the maximum allowed angular frequency and voltage amplitude deviations. P_{max} and Q_{max} are the maximum allowed active power and reactive power of the DC/AC converter of the SST.

As the d-axis of the PLL is aligned to the grid voltage, the reactive power droop control generates the d-axis AC voltage reference $v_{f,lv,dref}$, as illustrated in the reactive power control block in Fig. 5. Meanwhile, with the additional Syn v_0 block, the voltage reference of the reactive power droop controller can be smoothly moved from $v_{f,lv,ref}$ to v_g in grid synchronisation.

Due to the existence of the PLL and inner AC voltage control loop, in the proposed design, the active power droop control directly generates the q-axis voltage reference $v_{f,lv,qref}$, as illustrated in the active power control block in Fig. 5, as:

$$v_{f,lv,qref} = k_{pp} \left(P_{sst,ref} - P_{sst} \right) \tag{5}$$

wherein, k_{pp} is the droop coefficient.

In such as design, when the active power output of SST needs to change, the q-axis voltage of the converter output will be changed accordingly, which effectively change the phase of the converter output AC voltage. Consequently, the phase shift between the converter output and AC network changes which leads to the change of the SST active power output. For example, when $P_{sst} < P_{sst,ref}$ (i.e., P_{sst} needs to be increased and $v_{f,lv,qref} > 0$), the following control actions are taking place:

- The droop controller produces a positive $v_{f,lv,qref}$ for the voltage control, illustrated in Fig. 5.
- As $v_{f,lv,q}$ is zero due to the action of PLL, the AC voltage controller produces a q-axis current order such that a transient positive $v_{f,lv,q}$ is created.
- The positive $v_{f,lv,q}$ will lead the acceleration of the phase of the converter output, resulting in increased SST active power output P_{sst}.
- The action will only stop when $P_{sst} = P_{sst,ref}$.

Similarly, when $P_{sst} > P_{sst,ref}$ (i.e., P_{sst} needs to be reduced and $v_{f,lv,qref} < 0$), the droop controller produces a negative $v_{f,lv,qref}$ and a transient negative $v_{f,lv,q}$. Thus, the decelerated phase of the converter output voltage leads to P_{sst} reduction.

4.3 Active and reactive power coupling

The operation of the Q_{sst} - $v_{f,lv,d}$ and P_{sst} - $v_{f,lv,q}$ droop control makes the active and reactive power of SST strongly coupled. This is because the change of reactive power will lead to the change of d-axis voltage and through the AC voltage control loop, d-axis current (active current) will change accordingly which also result in the change of active power. Similarly, the change of active power will eventually lead to the change of q-axis current (reactive current) through the q-axis AC voltage loop and thus affecting the reactive power.

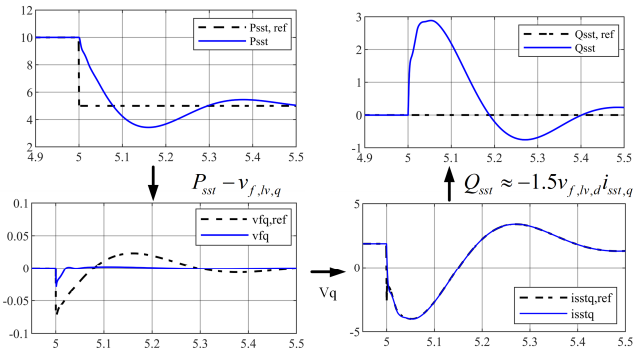

Fig. 6 SST active and reactive power coupling when $P_{sst,ref}$ is reduced

As an example, selected waveforms during step changes of active and reactive power references are shown in Fig. 6 and

Fig. 7, respectively. Considering the case when $P_{sst,ref}$ is reduced shown in Fig. 6, the active power error produces a negative $v_{f,lv,qref}$ through the droop coefficient k_{pp} in the P_{sst}-$v_{f,lv,q}$ droop controller. The negative q-axis voltage reference $v_{f,lv,qref}$ is fed to the q-axis voltage controller and results in a negative q-axis current reference $i_{sst,qref}$ as seen in Fig. 6. Considering the high dynamics of the current controller compared to the voltage and power controllers, the q-axis current immediately tracks the reference, which results in the fluctuation of Q_{sst}.

Similarly, as shown in Fig. 7, when $Q_{sst,ref}$ is increased, the reactive power error produces a positive $v_{f,lv,dref}$ which is fed to the d-axis voltage controller. A positive d-axis current reference $i_{sst,dref}$ is produced and considering the high dynamics of the current controller, the d-axis current immediately tracks the reference before, which results in the fluctuation of P_{sst}.

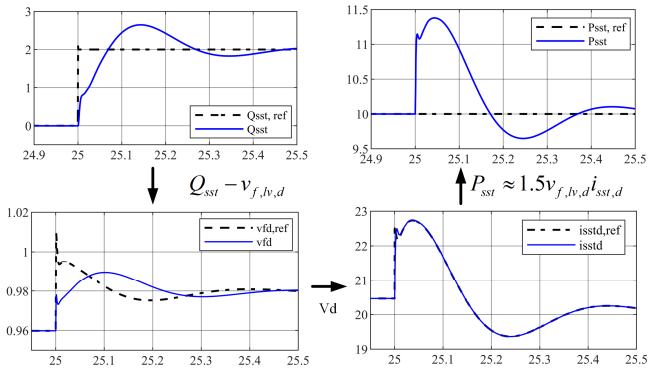

Fig. 7 SST active and reactive power coupling when $Q_{sst,ref}$ is increased

3.4 Proposed additional compensation control

From the above discussion, the coupling between P_{sst} and Q_{sst} is caused by the need to change q-axis current when $P_{sst,ref}$ changes, whereas the d-axis current has to be changed when $Q_{sst,ref}$ changes. To reduce the coupling between P_{sst} and Q_{sst}, a compensation control is proposed, as shown in Fig. 8. In essence, the additional active and reactive power feedforward terms are added directly to the d- and q-axis current components, such that the changes of $P_{sst,ref}$ and $Q_{sst,ref}$ can result in direct changes of active and reactive current, respectively. As shown, the active power compensation controller takes the active power error ΔP_{sst} as the input and generates an additional d-axis current reference $i_{sst,comd}$ by a gain k_{pid}, as:

$$i_{sst,comd} = k_{pid} \Delta P_{sst} \tag{6}$$

Similarly, the reactive power compensation controller takes the reactive power error ΔQ_{sst} as the input and generates the additional q-axis current reference $i_{sst,comq}$ by a gain k_{qiq}, as:

$$i_{sstqcom} = k_{qiq} \Delta Q_{sst} \tag{7}$$

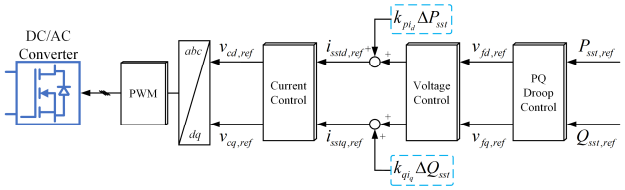

Fig. 8 Proposed compensation control scheme.

Consequently, when the SST changes active power reference, the active current will be immediately changed in addition to the effect of the normal P_{sst} - $v_{f,lv,q}$ control loop which advances the phase of the converter output through the q-axis voltage. As a result, the reactive power fluctuation is greatly reduced due to the reduced q-axis current demand from the P_{sst} - $v_{f,lv,q}$ controller. The effect during SST reactive power change can be described in a similar way but is not detailed here due to space limitation.

Table 1 Main parameters of the tested network

Parameter	Value
Rated power of SST	10 MW
Rated voltage at Bus 1 (connect to LFT)	0.96 pu
Rated voltage at Bus 2 (connect to SST)	1 pu
LVAC Load 1	(6 MW, 0 MVar)
LVAC Load 2	(10 MW, 0 MVar)
Bus 1 grid frequency f_g	49.5 Hz
SST AC frequency f_{lv} (when CNOP opens)	50 Hz

4 Simulation Results

The proposed control scheme of SST is tested with the network in Fig. 1, and the main parameters of the tested network and SST are listed in Table 1.

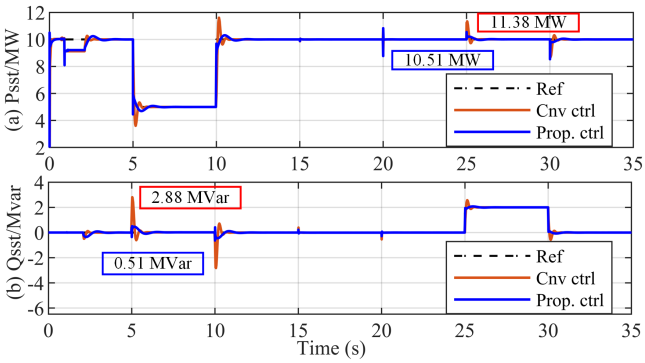

Fig. 9 Performance of system with conventional control and proposed compensation control: (a) SST active power; (b) SST reactive power.

Fig. 9 illustrates the performance of SST with the normal active and reactive power control and the proposed compensation control. In the study, k_{pid} = 0.008, and k_{qiq} = -0.0015. When simulation starts, the CNOP opens and SST supplies 10 MW to AC Load 2. It then starts synchronisation procedure to prepare CNOP closing. The CNOP closes at t = 2.1 s and immediately, the active and reactive power controller start to regulate the power output of SST to the active and reactive power references of 10 MW and 0 MVar. When the active power reference of the SST reduces from 10 MW to 5MW at t = 5 s, the active power quickly follows the order but significant reactive power variation is also induced as can be seen in Fig. 9. However, with the proposed compensation control, the maximum reactive power variation is reduced from 2.88 MVar (with conventional control) to 0.51 MVar, as illustrated in Fig. 9(b). Similar, when the reactive power reference of the SST increases from 0 MVar to 2 MVar at t = 25 s, the maximum active power variation is reduced from 1.72 MW (with conventional control) to 0.35 MW (with proposed

compensation control), as illustrated in Fig. 9(a). Similar performance can also be observed at t = 10 s and 30 s during active and reactive power reference changes. In addition, a 2 MW load shedding is applied to AC Load 2 at t = 15 s and the 2 MW load is added back to AC Load 2 at t = 20 s. The power outputs of the SST only see some small disturbances but quick track the references, as illustrated in Fig. 9(a)(b).

Fig. 10 and Fig. 11 illustrate the effect of different k_{pid} and k_{qiq} on the compensation control performance. In Fig. 10, the reactive power fluctuation at t = 5 s is illustrated when $P_{sst,ref}$ decreases from 10 to 5 MW. As can be seen in Fig. 10, the reactive power peak value reaches the minimum when k_{qiq} is selected as -0.015, though lower k_{qiq} (more negative) results in slower active power response. Similarly, as seen from Fig. 11, $Q_{sst,ref}$ increases from 0 to 2 MVar at t = 5 s, the active power fluctuation can be reduced by increasing k_{pid}. However, higher k_{pid} leads to slower reactive power response. Thus, k_{qiq} = -0.0015 and k_{pid} = 0.008 were selected as they provided balanced response for both active and reactive power.

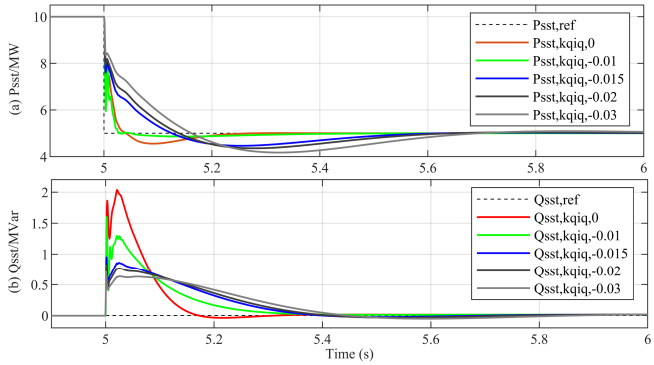

Fig. 10 Performance with different compensation control coefficients when active power reference changes: (a) SST output active power; (b) SST output reactive power.

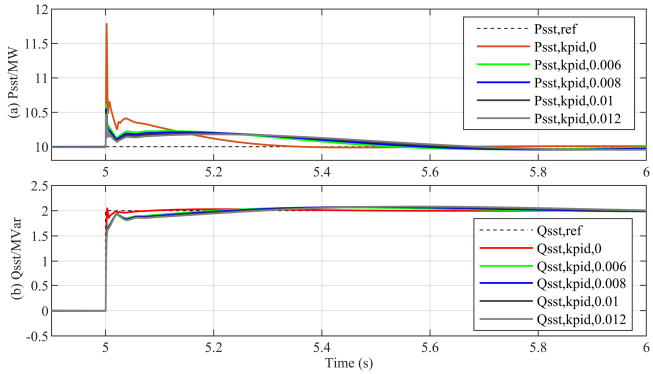

Fig. 11 Performance with different compensation control coefficients when reactive power reference changes: (a) SST output active power; (b) SST output reactive power.

5 Conclusion

A universal grid forming control scheme for SST to operate in the distribution network with the additional compensation control is proposed in this paper. A grid forming control structure is implemented for both island and grid connected operation of the SST LV network, such that control mode switch can be avoided. The active and reactive power feedforward terms are added directly to d- and q-axis current components to reduce the coupling between active and reactive power of SST brought by the droop control. The proposed compensation control can effectively reduce the coupling between active and reactive power during transients without affecting the overall system response. Simulation results validate the proposed compensation control.

7 References

[1] X. Liang, "Emerging Power Quality Challenges Due to Integration of Renewable Energy Sources," *IEEE Transactions on Industry Applications,* vol. 53, no. 2, pp. 855-866, 2017.

[2] J. Chen *et al.*, "Impact of smart transformer voltage and frequency support in a high renewable penetration system," *Electric Power Systems Research,* vol. 190, p. 106836, 2021/01/01/ 2021.

[3] A. Ghosh and A. Joshi, "The concept and operating principles of a mini custom power park," *IEEE Transactions on Power Delivery,* vol. 19, no. 4, pp. 1766-1774, 2004.

[4] S. Weckx, C. Gonzalez, and J. Driesen, "Combined Central and Local Active and Reactive Power Control of PV Inverters," *IEEE Transactions on Sustainable Energy,* vol. 5, no. 3, pp. 776-784, 2014.

[5] X. She, A. Q. Huang, S. Lukic, and M. E. Baran, "On integration of solid-state transformer with zonal DC microgrid," *IEEE Transactions on Smart Grid,* vol. 3, no. 2, pp. 975-985, 2012.

[6] A. Milczarek and M. Malinowski, "Comparison of Classical and Smart Transformers Impact on MV Distribution Grid," *IEEE Transactions on Power Delivery,* vol. 35, no. 3, pp. 1339-1347, 2020.

[7] S. Giacomuzzi, M. Langwasser, G. D. Carne, G. Buja, and M. Liserre, "Smart transformer-based medium voltage grid support by means of active power control," *CES Transactions on Electrical Machines and Systems,* vol. 4, no. 4, pp. 285-294, 2020.

[8] R. Zhu and M. Liserre, "Grid-Forming Control of Smart Solid-State Transformer in Meshed Network," in *2021 IEEE 12th International Symposium on Power Electronics for Distributed Generation Systems (PEDG)*, 2021, pp. 1-5.

[9] D. Das, V. M. H, C. Kumar, and M. Liserre, "Smart Transformer Enabled Meshed Hybrid Distribution Grid," *IEEE Transactions on Industrial Electronics,* pp. 1-1, 2020.

[10] A. Agrawal, C. S. Nalamati, and R. Gupta, "Hybrid DC–AC Zonal Microgrid Enabled by Solid-State Transformer and Centralized ESD Integration," *IEEE Transactions on Industrial Electronics,* vol. 66, no. 11, pp. 9097-9107, 2019.

[11] L. Xu, L. Yao, and C. Sasse, "Grid integration of large DFIG-based wind farms using VSC transmission," *IEEE Transactions on Power Systems,* vol. 22, no. 3, pp. 976-984, 2007.

[12] B. Zhao, Q. Song, W. Liu, and Y. Sun, "Overview of Dual-Active-Bridge Isolated Bidirectional DC–DC Converter for High-Frequency-Link Power-Conversion System," *IEEE Transactions on Power Electronics,* vol. 29, no. 8, pp. 4091-4106, 2014.

[13] J. M. Guerrero, J. C. Vasquez, J. Matas, L. G. d. Vicuna, and M. Castilla, "Hierarchical Control of Droop-Controlled AC and DC Microgrids—A General Approach Toward Standardization," *IEEE Transactions on Industrial Electronics,* vol. 58, no. 1, pp. 158-172, 2011.